

Regularity of Bunimovich's stadia

N. Chernov¹ and H.-K. Zhang²

Abstract

Stadia are popular models of chaotic billiards introduced by Bunimovich in 1974. They are analogous to dispersing billiards due to Sinai, but their fundamental technical characteristics are quite different. Recently many new results were obtained for various chaotic billiards, including sharp bounds on correlations and probabilistic limit theorems, and these results require new, more powerful technical apparatus. We present that apparatus here, in the context of stadia, and prove 'regularity' properties.

Keywords: Billiards, stadium, hyperbolicity, chaos, absolute continuity, distortion bounds.

1 Introduction

A billiard is a mechanical system in which a point particle moves in a compact container Q and bounces off its boundary ∂Q ; in this paper we only consider planar billiards. The billiard flow preserves a uniform measure on its phase space, and the corresponding collision map (generated by the collisions of the particle with the boundary, see below) preserves a natural (and often unique) absolutely continuous measure on its own phase space. The dynamical properties of a billiard are determined by the shape of the boundary, and they may vary greatly from completely regular (integrable) to strongly chaotic.

Generally speaking, the boundary of a billiard table may consist of curves of three types: convex inward (also called dispersing), convex outward (also

¹Department of Mathematics, University of Alabama at Birmingham, AL, 35294, USA; Email: chernov@math.uab.edu;

²Department of Mathematics and Physics, North China Electric Power University, Baoding, Hebei, 071003, CHINA; Email: hongkunuz@gmail.com

called focusing), and flat (called neutral). Sinai showed [S] that billiards with all-dispersing boundary are always strongly chaotic; precisely they are hyperbolic, ergodic, mixing, and have positive entropy. Billiards with all-flat boundary, i.e. polygons, are never hyperbolic: all of their Lyapunov exponents are zero; hence their entropy vanishes. Even though billiards in generic polygons are ergodic [KMS], they never possess strong statistical properties.

Billiards with focusing (convex) boundary components are much more diverse. It is an elementary fact that billiards in ellipses are completely regular (integrable). (Birkhoff conjectured that elliptic billiards were the *only* integrable convex billiards, but this yet remains to be proven.) Lazutkin [L] showed that billiards in generic strictly convex domains with smooth enough boundary had caustics, hence they could not be ergodic.

On the other hand, L. Bunimovich [B1, B2, B3] constructed chaotic billiards with convex (though not strictly convex) boundary. He also described a class of chaotic billiards with some focusing boundary components which may contain other (dispersing and flat) components as well. The most celebrated example is his stadium (a table bounded by two identical semicircles and two parallel lines); it has been subject to subsequent numerous studies by mathematicians and physicists.

Bunimovich showed that his billiards were hyperbolic, ergodic, and Bernoulli. Later Markov partitions were constructed [BSC1] and a central limit theorem for a suitable reduced collision map was proved [BSC2]. For the stadium, rates of the decay of correlations were estimated from above [CZ1, CZ2] and below [BG], and a non-classical central limit theorem for the (non-reduced) collision map was derived in [BG].

Many other billiards with focusing boundaries that have hyperbolic behavior were discovered later by Wojtkowski [W], Markarian [M], again Bunimovich [B4], and Donnay [D]. But beyond hyperbolicity, very little is known about these systems. In several cases ergodicity is proved [B2, Sz], too, and correlation rates estimated [CZ1], but a lot more needs to be done. One of the reasons for slow progress in these studies, perhaps, is the lack of adequate technical tools.

Many studies of ergodic and statistical properties of chaotic billiards use certain standard technical apparatus: distortion bounds, curvature bounds, absolute continuity (this includes estimates on the Jacobian of the holonomy map), and approximation of stable/unstable manifolds by continued fractions. For Sinai billiards, this machinery has been well developed; detailed

exposition (with complete proofs) can be found in [S, BSC1, BSC2, C1, C2] and in the book [CM].

The situation with Bunimovich’s billiards is different: they were studied *after* Sinai billiards, and it was often assumed that their basic technical characteristics were identical to those of Sinai billiards, so detailed proofs were not deemed necessary (only some fragmental arguments were given in [B1, B2, BSC1, BSC2], but they left out many details). For more general chaotic billiards with focusing boundaries (due to Wojtkowski, Markarian, and Donnay), the above technical tools are essentially undeveloped.

An attempt to undertake a systematic analysis of basic technical characteristics of Bunimovich’s billiards was recently made in [CM, Chapter 8], but it turned out that full proofs tend to be much longer and more involved than those known for Sinai billiards (for example, the mere approximation of stable and unstable manifolds by continued fractions took about 10 pages in [CM, Chapter 8]). Such complexity of Bunimovich’s billiards is hardly surprising as they are much more diverse than Sinai’s (strictly speaking, they include Sinai billiards as a *very* particular case). For this reason most of the analysis in the book [CM] was restricted to one model – the stadium, other types of Bunimovich’s billiards had to be left out.

Many results of [CM, Chapter 8] are new, but published only in the middle of a large book. Here we present them in a self-contained form of a research article; we hope that it will serve as a basis for further investigation of statistical properties of chaotic billiards with focusing boundary. In addition to the (classical, or ‘straight’) stadium, we extend our analysis to a nice but somewhat forgotten example – a ‘titled’ stadium, or a ‘squash’. It was originally proposed by Bunimovich (unpublished), investigated numerically in [FKCD], and later rediscovered in [CZ1], where it was called a ‘drivebelt table’.

2 Preliminaries

Here we recall basic facts about stadia, see [CM, Chapter 8] for more details. A stadium is a table bounded by two line segments tangential to two circular arcs. Bunimovich’s straight stadium, see Fig. 1(a), is made by two equal semicircles; it was introduced in 1974 [B2] but became popular in 1979 after the publication of his other article [B3]. A tilted, or drive-belt stadium, see Fig. 1(b), is bounded by two non-parallel lines and two arcs, one bigger than

the other. Notice that both stadia have C^1 , but not C^2 , boundary. They remain chaotic no matter how short the parallel segments are; but if they vanish, the stadia turn into disks where the billiards are completely integrable. Thus one gets continuous families of billiard tables where a transition from a completely regular region to total chaos occurs instantly.



Figure 1: Straight stadium (a) and drive-belt stadium (b).

Let $\mathcal{D} \subset \mathbb{R}^2$ be a stadium. Its boundary can be decomposed as

$$\partial\mathcal{D} = \partial^0\mathcal{D} \cup \partial^-\mathcal{D},$$

where $\partial^-\mathcal{D} = \Gamma_1 \cup \Gamma_2$ denotes the union of two arcs, and $\partial^0\mathcal{D} = \Gamma_3 \cup \Gamma_4$ consists of straight sides of \mathcal{D} . Let $\mathcal{M} = \partial\mathcal{D} \times [-\pi/2, \pi/2]$ be the standard cross-section of the billiard dynamics, we call \mathcal{M} the *collision space*. Canonical coordinates on \mathcal{M} are r and φ , where r is the arc length parameter on $\partial\mathcal{D}$ and $\varphi \in [-\pi/2, \pi/2]$ is the angle of reflection. The first return map $\mathcal{F} : \mathcal{M} \rightarrow \mathcal{M}$ is called the *collision map* or the *billiard map*, it preserves smooth measure $d\mu = \cos \varphi dr d\varphi$ on \mathcal{M} . The collision space can be naturally divided into focussing and neutral parts:

$$\mathcal{M}_- = \{(r, \varphi) : r \in \partial^-\mathcal{D}\}, \quad \mathcal{M}_0 = \{(r, \varphi) : r \in \partial^0\mathcal{D}\}.$$

To avoid unnecessary complications for the drive-belt table, we assume that the larger arc Γ_1 has length

$$(2.1) \quad |\Gamma_1| = (\pi + \omega)\mathbf{r}, \quad \omega \in (0, \pi/3].$$

This guarantees that there are no periodic orbits with more than 2 reflections off the arc Γ_1 . We believe that our results can be extended beyond this restriction with a little extra work.

We will use two metrics in the space \mathcal{M} : the standard Euclidean metric $\|(dr, d\varphi)\|^2 = (dr)^2 + (d\varphi)^2$ and a special billiard-related p-metric $\|(dr, d\varphi)\|_p = \cos \varphi |dr|$. The latter is a version of adapted metrics, in which the given hyperbolic map expands unstable tangent vectors monotonically, see [CM, Sections 4.4 and 8.2].

We recall that every smooth curve $\gamma \subset \mathcal{M}$ produces a smooth family of (outgoing) directed lines leaving $\partial\mathcal{D}$; as well as a family of (incoming) directed lines falling onto $\partial\mathcal{D}$. Tangent vectors $u \in T_x\mathcal{M}$ correspond to infinitesimal bundles of directed lines. An orthogonal cross section of such a bundle of directed lines, equipped with properly directed unit normal vectors, is called a *wave front*. Its curvature (i.e. the curvature of its cross-section) is related to the slope of the corresponding tangent vector in \mathcal{M} .

Suppose an infinitesimal wave front collides with $\partial\mathcal{D}$ at a point $x = (r, \varphi)$. Denote its precollisional and postcollisional curvature by \mathcal{B}^- and \mathcal{B}^+ , respectively (as usual, it is assumed that divergent wave fronts have positive curvature and convergent fronts negative). The front induces a tangent vector $(dr, d\varphi) \in T_x\mathcal{M}$ whose slope $\mathcal{V} = d\varphi/dr$ is given by:

$$(2.2) \quad \mathcal{V} = \mathcal{B}^- \cos \varphi + \mathcal{K} = \mathcal{B}^+ \cos \varphi - \mathcal{K},$$

where \mathcal{K} denotes the curvature of the boundary $\partial\mathcal{D}$ at the point x . For flat boundaries $\mathcal{K} = 0$, and for a circular arc of radius \mathbf{r} we set $\mathcal{K} = -1/\mathbf{r}$ (the negative sign here is just due to traditions in the literature.)

The dynamics of wave fronts plays a crucial role in the analysis of hyperbolic billiards as it describes the transformation of tangent vectors to \mathcal{M} .

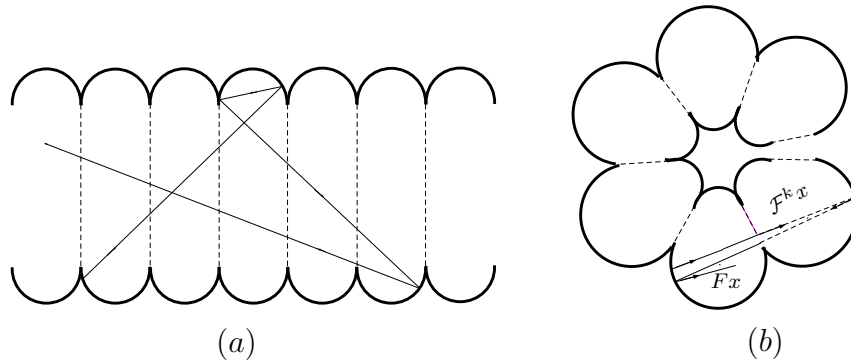


Figure 2: Infinite tables made by identical stadia with common flat sides.

If the billiard table has flat sides, it is common to reflect it across its flat sides so that the trajectories ‘run through’ the flat sides into the mirror images of the table, as if the flat sides were transparent. This transformation of billiard trajectories is called *unfolding*. In the stadia, it is particularly simple, see below.

Due to a natural symmetry, the mirror image of a straight stadium \mathcal{D} across its flat side is identical to \mathcal{D} itself. Further images make an infinite row of identical stadia with common flat sides; see Fig. 2 (left). Thus we obtain an unbounded billiard table \mathcal{D}_∞ whose border consists of two sets of identical adjacent arcs. Observe that \mathcal{D}_∞ has no flat boundary component; all collisions occur at arcs only. A similar picture for the skewed stadium is shown in Fig. 2 (right).

In stadia, there are three types of long series of nonessential collisions (see illustration in Fig. 3):

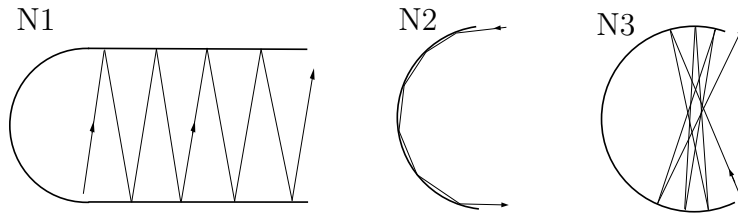


Figure 3: Three types of nonessential collisions.

Type N1. Collisions occur at flat boundary components only. The unfolding procedure transforms the corresponding trajectories into straight lines along which the particle moves without collisions; thus they behave as collision-free orbits in billiards with infinite horizons.

Type N2. Collisions occur at one focusing arc and $|\varphi| \approx \pi/2$. In this case the trajectory is almost tangent to the arc, as it ‘slides’ along the arc. Such series of collisions are said to be *sliding*.

Type N3. Collisions occur at one focusing arc and $|\varphi|$ is near 0. In this case the trajectory is close to a periodic orbit running along a diameter of the corresponding arc; we call such series *diametrical* (they can occur only on a focusing arc larger than half-circle).

In order to reduce nonessential collisions, we redefine the map \mathcal{F} so that in every series of collisions with a focusing arc only the very first and the very

last ones will be kept. Accordingly, we define a subset $\mathcal{M}_\diamond \subset \mathcal{M}$ consisting of points $x = (q, v)$ such that q belongs to a semicircle and either its image $\mathcal{F}(x)$ or its preimage $\mathcal{F}^{-1}(x)$ does not lie on that same semicircle. (For the drive-belt table, we also remove points $x = (q, v)$ such that q lies on the larger arc Γ_1 , the two points $\mathcal{F}^{\pm 1}x$ lie on a flat side, and both points $\mathcal{F}^{\pm 2}x$ lie on Γ_1 again; such points and the need for their removal are described in [CZ1, p. 1551].)

Also, we consider the return map $\mathcal{F}_\diamond: \mathcal{M}_\diamond \rightarrow \mathcal{M}_\diamond$; i.e. $\mathcal{F}_\diamond(x) = \mathcal{F}^{n(x)}(x)$ where $n(x) = \min\{n > 0: \mathcal{F}^n(x) \in \mathcal{M}_\diamond\}$. The map \mathcal{F}_\diamond preserves the measure μ conditioned on \mathcal{M}_\diamond , which we denote by $\mu_\diamond = [\mu(\mathcal{M}_\diamond)]^{-1}\mu$. The set \mathcal{M}_\diamond consists of two hexagons (corresponding to two arcs) for the straight stadium; fig. 4(a) shows one hexagon corresponding to the semi-circle Γ_1 . For the drive-belt, the region is a more complicated polygon, see Fig. 4(b).

The parallelogram $CBDE$ (or $C'BD'E$) contains all the points of the *first* collisions with the arc and $ACGD$ (or $AC''GD''$) contains all the points of the *last* collisions with the arc (their intersection, the rhombus $CHDI$, consists of points of *only* collisions with the arc). The dark triangles contain points of intermediate collisions, so they are not included in \mathcal{M}_\diamond .

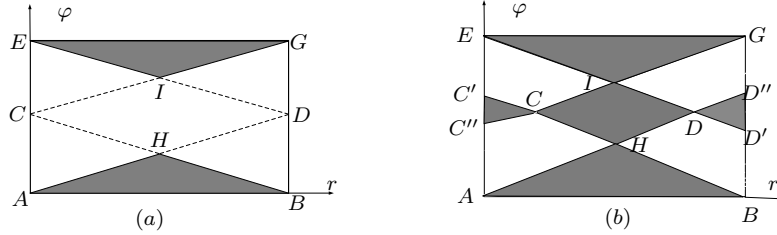


Figure 4: The set \mathcal{M}_\diamond .

The map \mathcal{F}_\diamond takes the white region CEI (or $C'EIC$) onto the white region DGI (or $D''GID$); likewise, it takes BHD ($BHDD'$) into ACH ($AC''C'H$).

Next we describe the action of \mathcal{F}_\diamond on the upper left white region. On the bigger triangle CEG (or $C''EG$), the original map \mathcal{F} acts by the rule

$$(2.3) \quad (r, \varphi) \mapsto (r + \mathbf{r}(\pi - 2\varphi), \varphi);$$

If a billiard trajectory makes k successive collisions with an arc (along which the φ coordinate remains unchanged), then

$$(2.4) \quad \varphi = \frac{\pi}{2} - \frac{|\Gamma_1|}{2k\mathbf{r}} + \mathcal{O}\left(\frac{1}{k^2}\right), \quad \text{so} \quad \cos \varphi = \frac{|\Gamma_1|}{2k\mathbf{r}} + \mathcal{O}\left(\frac{1}{k^2}\right).$$

Now the new map \mathcal{F}_\diamond acts by the rule

$$(2.5) \quad r \mapsto r + k\mathbf{r}(\pi - 2\varphi).$$

It is linear on each region where k is constant, but there are countably many such regions in CEI (or $CIEC'$) corresponding to different k 's; they are separated by lines consisting of trajectories hitting the endpoint of our arc on their last collision with it. So the new map \mathcal{F}_\diamond is piecewise linear and has countably many discontinuity lines.

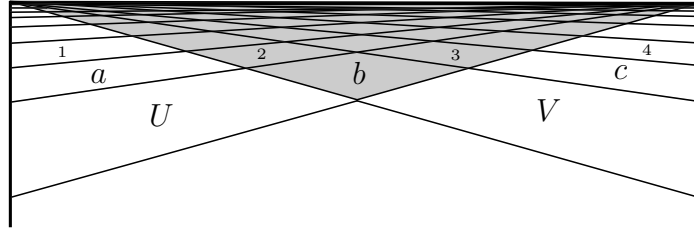


Figure 5: The action of \mathcal{F}

The action of \mathcal{F} and \mathcal{F}_\diamond in the upper region $CEGD$ (or $C'EGD''$) is shown in Fig. 5. It is divided by two families of straight lines, each family converging to one top corner of the hexagon, into countably many quadrilaterals that make a checkerboard pattern. The original billiard map \mathcal{F} transforms every quadrilateral (linearly) into the next one on the right in the same horizontal row. The new map \mathcal{F}_\diamond sends the leftmost quadrilateral onto the rightmost one in the same row. This is illustrated by the following diagram (see Fig. 5):

\mathcal{F}	\mathcal{F}_\diamond
$U \mapsto V$	$U \mapsto V$
$a \mapsto b \mapsto c$	$a \mapsto c$
$1 \mapsto 2 \mapsto 3 \mapsto 4$	$1 \mapsto 4$

Observe that the lines in the upper left white region are singularities for the map \mathcal{F}_\diamond , while those in the upper right white region are singularities

for its inverse $\mathcal{F}_\diamond^{-1}$. The number of quadrilaterals in each row equals k (the number of successive collisions with Γ_1). The lower white regions in $ABDC$ (or $ABD'C''$) are divided into quadrilaterals in a similar manner, but the maps \mathcal{F} and \mathcal{F}_\diamond move them from right to left.

The map \mathcal{F}_\diamond has other singularities which make two symmetric families of self-similar increasing lines accumulating near the vertices C and D , see Fig. 6. In the straight stadium, these singularities are caused by trajectories bouncing between the two flat sides while moving slowly from one arc to the other and eventually hitting an endpoint of the latter. In the drive-belt, the singularities are caused by near-diametrical trajectories bouncing around inside the larger arc and eventually hitting its endpoint. These singularities are described in [CM, Section 8.8] and [CZ1, p. 1551]. If we number the singularity lines as they approach the vertices C and D , then the n th line will be $\mathcal{O}(1/n)$ away from the limit vertex, and the distance between the n th and $(n + 1)$ st line will be $\mathcal{O}(1/n^2)$.

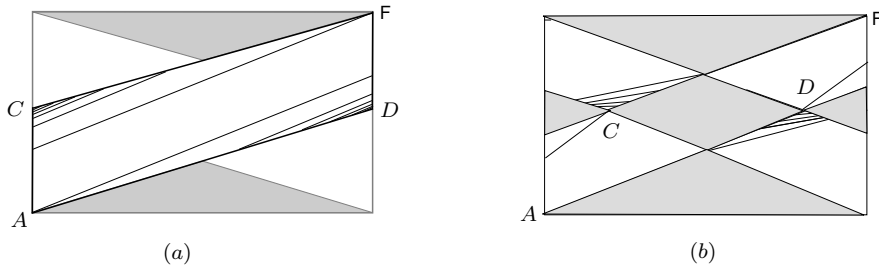


Figure 6: The singularities of \mathcal{F}_\diamond near C and D : (a) stadium and (b) drive-belt.

3 Hyperbolicity

Here we use stable and unstable fronts to describe the hyperbolicity of stadia. Mostly we deal with unstable fronts, but due to the time reversibility stable fronts have all similar properties. We say that the colliding wave front and the corresponding tangent vector are *unstable* if

$$(3.1) \quad \mathcal{B}^- \in \left(0, \frac{1}{\mathbf{r} \cos \varphi}\right)$$

whenever $\mathcal{K} = -1/\mathbf{r} < 0$.

Denote by $\mathcal{C}_x^u \subset \mathcal{T}_x\mathcal{M}$ the unstable cone at $x \in \mathcal{M}$, i.e. the closure of the set of all unstable tangent vectors for focusing arcs:

$$\mathcal{C}_x^u = \{(dr, d\varphi) \in \mathcal{T}_x\mathcal{M} : -1/\mathbf{r} \leq d\varphi/dr \leq 0\}.$$

In this section we prove that the return map $\mathcal{F}_\diamond: \mathcal{M}_\diamond \rightarrow \mathcal{M}_\diamond$ for any stadium is uniformly hyperbolic. Given a point $x = (r, \varphi) \in \mathcal{M}_\diamond$, we denote by $x_n = (r_n, \varphi_n) = \mathcal{F}_\diamond^n(x)$ its images, by t_n the collision time at the point x_n , and by $\tau_n = t_{n+1} - t_n$ the intervals between collisions. Also let \mathcal{K}_n denote the curvature of $\partial\mathcal{D}$ at the point x_n and $\mathcal{R}_n = 2\mathcal{K}_n/\cos\varphi_n$ the so called ‘collision parameter’. Note that n here is the counter of essential collisions only.

Given a tangent vector $dx = (dr, d\varphi) \in \mathcal{T}_x\mathcal{M}_\diamond$, we denote by $dx_n = (dr_n, d\varphi_n) = D_x\mathcal{F}_\diamond^n(dx)$ its image, by $\mathcal{V}_n = d\varphi_n/dr_n$ its slope, and by \mathcal{B}_n^\pm the curvature of the corresponding wave front before and after the collision; recall the relation (2.2). Also we denote by $\|dx_n\| = [(dr_n)^2 + (d\varphi_n)^2]^{1/2}$ the Euclidean norm and by $\|dx_n\|_p = |\cos\varphi_n dr_n|$ the so called p -norm of these tangent vectors. There two norms are clearly related by

$$\|dx_n\| = \frac{\|dx_n\|_p}{\cos\varphi_n} \sqrt{1 + \mathcal{V}_n^2}.$$

The following relations are standard in the theory of billiards for the original collision map \mathcal{F} (not the induced map \mathcal{F}_\diamond):

$$(3.2) \quad \frac{1}{\mathcal{B}_n^-} = \frac{1}{\mathcal{B}_{n-1}^+} + \tau_{n-1}, \quad \mathcal{B}_n^+ = \mathcal{B}_n^- + \mathcal{R}_n$$

and the expansion in the p -metric is given by

$$(3.3) \quad \frac{\|dx_{n+1}\|_p}{\|dx_n\|_p} = |1 + \tau_n \mathcal{B}_n^+| = \frac{|\mathcal{B}_n^+|}{|\mathcal{B}_{n+1}^-|}.$$

They also easily extend to the induced map \mathcal{F}_\diamond if all the nonessential collisions between x_n and x_{n+1} occur at flat components of the boundary (according to type N1, see above), cf. [BSC2, CM]. The following lemma extends these relations to the induced map \mathcal{F}_\diamond in the presence of types N2 and N3 nonessential collisions (but we have to slightly redefine τ_n and \mathcal{R}_n):

Lemma 3.1. *Suppose x_n and x_{n+1} are the first and, respectively, the last collision in a series of collisions at the same circular arc. Then (3.2) and (3.3) hold if we set $\tau_n = -(t_{n+1} - t_n)$ and $\mathcal{R}_n = \mathcal{K}_n/\cos\varphi_n$.*

Proof. We give a brief argument here, see [CM, Section 8.7] for a more detailed and pictorial analysis, including the notion of ‘virtual trajectories’. Let an infinitesimal wave front move along the trajectory of x_n and experience $m + 1$ successive collisions with a circular arc of radius \mathbf{r} (the $(m + 1)$ st collision occurs at the point x_{n+1}). Let $x_n = y_0$, $\mathcal{F}^k x_n = y_k$, then $x_{n+1} = y_m$. Denote the precollisional and postcollisional curvature of y_k by $\bar{\mathcal{B}}_k^-$ and $\bar{\mathcal{B}}_k^+$, with $\bar{\mathcal{B}}_0^- = \mathcal{B}_n^-$ and $\bar{\mathcal{B}}_k^+ = \mathcal{B}_{n+1}^+$. It is easy to show for $k = 0, 1, \dots, m$

$$(3.4) \quad \bar{\mathcal{B}}_k^+ = \bar{\mathcal{B}}_k^- - \frac{4}{\tau}, \quad \frac{1}{\bar{\mathcal{B}}_{k+1}^-} = \frac{1}{\bar{\mathcal{B}}_k^+} + \tau$$

where $\tau = 2\mathbf{r} \cos \varphi_n$. Notice that

$$(3.5) \quad \begin{aligned} \bar{\mathcal{B}}_k^+ &= -4/\tau + \bar{\mathcal{B}}_k^- = -\frac{4}{\tau} + \frac{1}{\tau + \frac{1}{-\frac{4}{\tau} + \frac{1}{\tau + \dots \frac{1}{-\frac{4}{\tau} + \mathcal{B}_n^-}}} \\ &= -\frac{2}{\tau} + \frac{1}{-k\tau + \frac{1}{-\frac{2}{\tau} + \mathcal{B}_n^-}}. \end{aligned}$$

Especially, for $k = m$, we have

$$\mathcal{B}_{n+1}^+ = \bar{\mathcal{B}}_m^+ = -\frac{2}{\tau} + \frac{1}{-m\tau + \frac{1}{-\frac{2}{\tau} + \mathcal{B}_n^-}}.$$

Thus for x_n , the first in the series of $m + 1$ collisions, we set $\tau_n = -m\tau$ and $\mathcal{R}_n = \mathcal{R}_{n+1} = \mathcal{K}_n / \cos \varphi_n$, and obtain

$$(3.6) \quad \mathcal{B}_n^+ = \mathcal{R}_n + \mathcal{B}_n^-; \quad \frac{1}{\mathcal{B}_{n+1}^-} = \tau_n + \frac{1}{\mathcal{B}_n^+}; \quad \mathcal{B}_{n+1}^+ = \mathcal{R}_{n+1} + \mathcal{B}_{n+1}^-,$$

which implies (3.2). Next, the expansion factor in the p-metric is

$$(3.7) \quad \frac{\|dy_{k+1}\|_p}{\|dy_k\|_p} = |1 + \tau \bar{\mathcal{B}}_k^+| = \frac{|\bar{\mathcal{B}}_k^+|}{|\bar{\mathcal{B}}_{k+1}^-|}.$$

Then the expansion in the course of the whole series is

$$\frac{\|dx_{n+1}\|_p}{\|dx_n\|_p} = \prod_{k=0}^m |1 + \tau(-4/\tau + \bar{\mathcal{B}}_k^-)|,$$

which implies (3.3). □

In what follows, we use τ_n as defined in the above lemma, in particular $\tau_{\min} > 0$. In the case of drivebelt, we also have $\tau_{\max} < \infty$.

The slope $\mathcal{V} = d\varphi/dr$ of an unstable vector $(dr, d\varphi)$ is always negative; in fact, $-1/\mathbf{r} \leq \mathcal{V} < 0$ (see (2.2) and (3.1)). In what follows, we also suppose that its preimage $(dr_{-1}, d\varphi_{-1})$ is an unstable vector, too (this slightly reduces the size of unstable cones). Let x and x_{-1} belong to opposite arcs. It is standard for Bunimovich billiards [B1, B2, CM] that unstable wave fronts make convergent families of trajectories that focus between collisions and then become divergent; the key fact is that they travel longer as divergent fronts than they do as convergent fronts, i.e. the focusing point must lie closer to x_{-1} than to x ; it divides the interval τ_{-1} between x_{-1} and x in the ratio $\rho \leq 1 - c_0$, where $c_0 = c_0(\mathcal{D}) > 0$ is a constant. This implies

$$\frac{\|dx\|_p}{\|dx_{-1}\|_p} = \frac{|\mathcal{B}_{-1}^+|}{|\mathcal{B}^-|} = \rho^{-1} \geq (1 - c_0)^{-1} > 1.$$

Note also that $0 \leq \mathcal{B}^- \leq 2/\tau_{\min} = \text{const}$, and

$$(3.8) \quad \mathcal{B}^- \leq \frac{1 - c_1}{\mathbf{r} \cos \varphi},$$

where $c_1 = c_1(\mathcal{D}) > 0$ is a constant. Since the slope of our tangent vector is $\mathcal{V} = \mathcal{K} + \mathcal{B}^- \cos \varphi$ and $\mathcal{K} = -1/\mathbf{r} = \text{const}$, we have $-1/\mathbf{r} \leq \mathcal{V} \leq -c_1/\mathbf{r}$. This can be expressed as $\mathcal{V} \asymp -1$ (our notation $a \asymp b$ means $0 < C_1 < a/b < C_2 < \infty$ for some positive constants C_1, C_2 depending only on \mathcal{D}).

Now let x and x_{-1} belong to the same arc (they may be separated by other, nonessential, sliding or diametrical collisions). In that case we need to assume that the second preimage of our tangent vector $(dr_{-2}, d\varphi_{-2})$ is unstable, too, so that we can apply (3.8) to x_{-1} . This implies

$$\mathcal{B}_{-1}^+ = -\frac{1}{\mathbf{r} \cos \varphi_{-1}} + \mathcal{B}_{-1}^- \leq -\frac{c_1}{\mathbf{r} \cos \varphi_{-1}}$$

according to (3.5). As $\tau_{-1} \leq -\tau_{\min} < 0$, we have

$$\frac{\|dx\|_p}{\|dx_{-1}\|_p} = |1 + \tau_{-1}\mathcal{B}_{-1}^+| \geq 1 + \frac{c_1\tau_{\min}}{\mathbf{r} \cos \varphi_{-1}},$$

which is bounded away from 1.

If x is of type N2, the time τ_{-1} has the lower bound $\tau_{-1} \geq -\tau_{\max} > -\infty$, and it follows that

$$-\frac{1}{\tau_{\min}} \leq \mathcal{B}^- \leq -\frac{1}{\tau_{\max} + c_1/\mathbf{r}},$$

i.e. $\mathcal{B}^- \asymp -1$. If the number k of sliding collisions between the points x_{-1} and x is large, then $\cos \varphi \asymp 1/k$ due to (2.4) and

$$\mathcal{B}^+ = -\frac{1}{\mathbf{r} \cos \varphi} + \mathcal{B}^- \asymp -k.$$

If x is of type N3, the time τ_{-1} has the lower bound $\tau_{-1} \geq -c_2k > -\infty$, and it follows that

$$(3.9) \quad -\frac{1}{k\tau_{\min}} \leq \mathcal{B}^- \leq -\frac{1}{k\tau_{\max} + c_1/\mathbf{r}},$$

i.e. $\mathcal{B}^- \asymp -1/k$. Note that

$$\mathcal{B}^+ = -\frac{1}{\mathbf{r} \cos \varphi} + \mathcal{B}^- \asymp -1.$$

For the slope \mathcal{V} , we always have

$$\mathcal{V} = -\mathcal{K} + \mathcal{B}^+ \cos \varphi = \mathcal{B}^- \cos \varphi \asymp -1/k$$

(this can also be derived directly from (2.4)–(2.5)).

We summarize the above discussion. There is always a lower bound for the slope of unstable vectors

$$(3.10) \quad -\infty < \text{const} \leq \mathcal{V} < 0.$$

The expansion of unstable vectors in the p-metric is always uniform:

$$(3.11) \quad \frac{\|dx_{n+1}\|_p}{\|dx_n\|_p} = |1 + \tau_n \mathcal{B}_n^+| \geq \Lambda > 1,$$

where $\Lambda = \Lambda(\mathcal{D}) > 1$ is a constant. Moreover, when $\cos \varphi_n$ is small, a better estimate is available:

$$(3.12) \quad \frac{\|dx_{n+1}\|_p}{\|dx_n\|_p} = |1 + \tau_n \mathcal{B}_n^+| \asymp \frac{|\tau_n|}{\cos \varphi_n}.$$

For the expansion in the Euclidean metric we have

$$(3.13) \quad \frac{\|dx_n\|}{\|dx_0\|} = \frac{\|dx_n\|_p}{\|dx_0\|_p} \frac{\cos \varphi_0}{\cos \varphi_n} \frac{\sqrt{1 + \mathcal{V}_n^2}}{\sqrt{1 + \mathcal{V}_0^2}}.$$

The last fraction is uniformly bounded away from zero and infinity due to (3.10). To deal with the middle fraction, we use (3.12) with $n = 0$ and obtain

$$(3.14) \quad \frac{\|dx_n\|}{\|dx_0\|} \geq \text{const} \times \frac{\|dx_n\|_p}{\|dx_1\|_p} \geq \hat{c} \Lambda^n,$$

where $\hat{c} = \hat{c}(\mathcal{D}) > 0$ is a constant. Thus the hyperbolicity is uniform in the Euclidean metric, too. Note, however, that the expansion of unstable vectors is always monotone in the p-metric, but it may not be so in the Euclidean metric.

We also note that

$$(3.15) \quad \frac{\|dx_{n+1}\|}{\|dx_n\|} = \frac{\|dx_{n+1}\|_p}{\|dx_n\|_p} \frac{\cos \varphi_n}{\cos \varphi_{n+1}} \frac{\sqrt{1 + \mathcal{V}_{n+1}^2}}{\sqrt{1 + \mathcal{V}_n^2}} \asymp \frac{|\tau_n|}{\cos \varphi_{n+1}}$$

which is useful when $\cos \varphi_{n+1} \approx 0$.

There are four ‘problematic’ regions in the reduced collision space \mathcal{M}_\diamond where the quantities we deal with approach zero or infinity. These are the first and the last collisions in a long series of $k \gg 1$ sliding collisions with an arc. Also, these are collisions preceding a long series of $k \gg 1$ reflections off the flat sides of the original stadium and the first collisions in a long series of $k \gg 1$ diametrical collisions with the larger arc of the drivebelt table. Such points are located in the vicinities of the vertices A, B, E, G and C, D, respectively, in the hexagon in Fig. 4.

Table 1 presents asymptotic behavior (in the sense of \asymp) of various quantities at these three types of ‘problematic’ collisions (for example, at the first

collision type:	before a series of k reflections at flat sides	in a series of k sliding collisions:		in a series of k diametrical coll's:	
		first one	last one	first one	last one
τ	k	-1	1	$-k$	1
$\cos \varphi$	1	$1/k$	$1/k$	1	1
\mathcal{B}^-	$1/k$	1	-1	$1/k$	1
\mathcal{R}	-1	$-k$	$-k$	-1	1
\mathcal{B}^+	-1	$-k$	$-k$	-1	-1
$\mathcal{V} = d\varphi/dr$	-1	-1	$-1/k$	-1	$-1/k$
$ 1 + \tau\mathcal{B}^+ $	k	k	k	k	1

Table 1: Asymptotics of various quantities at five types of ‘problematic’ collisions.

sliding collision $\tau \asymp -1$, $\cos \varphi \asymp 1/k$, etc.). All the formulas in the table follow immediately from our previous analysis or from each other.

The last line in Table 1 describes the expansion of unstable curves in the p -metric, and now we describe it in the Euclidean metric. If $x \in \mathcal{M}_\diamond$ is the first sliding collision, then $\cos \varphi = \cos \varphi_1 (\asymp 1/k)$; hence $\|dx_1\|/\|dx\| \asymp k \asymp \|dx_1\|_p/\|dx\|_p$.

Let $x \in \mathcal{M}_\diamond$ be the last collision in a long series of $k \gg 1$ sliding collisions with an arc. Clearly, $\mathcal{F}_\diamond(x)$ is the first collision in another long series of $k_1 \gg 1$ of sliding collisions with the opposite arc. In fact, $c\sqrt{k} \leq k_1 \leq Ck^2$ for some constants $c, C > 0$.

Since $\cos \varphi_1 \asymp 1/k_1$, we obtain due to (3.15)

$$(3.16) \quad c\sqrt{k} \leq \|dx_1\|/\|dx\| \leq Ck^2$$

for some constants $c, C > 0$. Now let $x \in \mathcal{M}_\diamond$ precede a long series of $k \gg 1$ reflections off the flat sides of the original stadium or precede a series of k diametrical collisions with the larger arc of the drivebelt. Then $\mathcal{F}_\diamond(x)$ also precedes another long series of k_1 same type of non-essential collisions.

In [BSC1, BSC2, CZ1], it was shown for both cases, $cm \leq k_1 \leq Cm$ for

some constants $c, C > 0$. As a result for both cases, $\|dx_1\|/\|dx\| \asymp k \asymp \|dx_1\|_p/\|dx\|_p$.

4 Stable and unstable curves

Here we consider stable and unstable curves in the reduced collision space \mathcal{M}_\diamond of a stadium. Stable curves have positive slope and unstable curves have negative slope. These curves cannot self-intersect. Their lengths (in both metrics, $|\cdot|$ and $|\cdot|_p$) are uniformly bounded. If W^u is an unstable curve and W^s a stable curve, then their intersection $W^u \cap W^s$ is transversal and consists of at most one point.

We note that the singularity lines of the map \mathcal{F}_\diamond are increasing (stable) curves, so each unstable curve intersects every singularity line in at most one point. Thus the image $\mathcal{F}_\diamond(W)$ of any unstable curve $W \subset \mathcal{M}_\diamond$ is a finite or countable union of unstable curves, which we call the *components* of $\mathcal{F}_\diamond(W)$.

Now we establish the C^2 smoothness of these curves, with uniformly bounded second derivatives (for dispersing billiards, uniform bounds have been established for higher order derivatives as well [CM, Chapter 4], but here we do not go beyond the second derivative to avoid unnecessary complications). Our curves contain endpoints and the smoothness always extends to one-sided derivatives at those.

Proposition 4.1. *For every C^2 smooth unstable curve $W \subset \mathcal{M}_\diamond$ there is an $n_W \geq 1$ such that for all $n > n_W$ every smooth component $W' \subset \mathcal{F}_\diamond^n(W)$ has its second derivative uniformly bounded:*

$$(4.1) \quad |d^2\varphi_n/dr_n^2| \leq C$$

on W' , where $C = C(\mathcal{D}) > 0$ is a constant.

Proof. We will suppress the index n for brevity. Let $(r, \varphi(r))$ denote a point on W' . Differentiating (2.2) (in which $\mathcal{K} \equiv \text{const}$) gives

$$(4.2) \quad d^2\varphi/dr^2 = -\mathcal{B}^- \mathcal{V} \sin \varphi + \cos \varphi d\mathcal{B}^-/dr.$$

The first term is uniformly bounded; hence the second derivative would be bounded if we prove

$$(4.3) \quad |d\mathcal{B}^-/dr| \leq C'$$

on W' , where $C' = C'(\mathcal{D}) > 0$ is a constant.

Since W is C^2 smooth, $\sup_W |d^2\varphi/dr^2| < \infty$; hence

$$(4.4) \quad \sup_W |\cos \varphi \, d\mathcal{B}^-/dr| < \infty$$

due to (4.2). Using our standard notation, we have for $n \geq 1$

$$\frac{1}{\mathcal{B}_n^-} = \frac{1}{\mathcal{B}_{n-1}^+} + \tau_{n-1}, \quad \mathcal{B}_n^+ = \mathcal{B}_n^- + \mathcal{R}_n$$

hence differentiating both sides of above formula with respect to r_n gives

$$(4.5) \quad \begin{aligned} \frac{d\mathcal{B}_n^-}{dr_n} &= \left[\frac{\mathcal{B}_n^-}{\mathcal{B}_{n-1}^+} \right]^2 \frac{d\mathcal{B}_{n-1}^+}{dr_n} - [\mathcal{B}_n^-]^2 \frac{d\tau_{n-1}}{dr_n} \\ &= -[\mathcal{B}_n^-]^2 \frac{d\tau_{n-1}}{dr_n} + \left(\frac{\|dx_{n-1}\|_p}{\|dx_n\|_p} \right)^2 \left(\frac{d\mathcal{R}_{n-1}}{dr_n} + \frac{d\mathcal{B}_{n-1}^-}{dr_n} \right). \end{aligned}$$

First we check that

$$(4.6) \quad |d\tau_{n-1}/dr_n| \asymp 1,$$

which is straightforward for type N1 collisions. A different case appears when x_{n-1} is the first collision in a type N2 series of k collisions with an arc. Then $|\tau_{n-1}| = 2(k-1)\mathbf{r} \cos \varphi_n$; hence

$$\frac{d\tau_{n-1}}{dr_n} = -2(k-1)\mathbf{r} \sin \varphi_n \cdot \mathcal{V}_n$$

Notice that $|\mathcal{V}_n| \asymp 1/k$. So $\frac{d\tau_{n-1}}{dr_n}$ is uniformly bounded. Thus the first term in (4.5) is always uniformly bounded.

Next

$$\frac{d\mathcal{R}_{n-1}}{dr_n} = \frac{d\mathcal{R}_{n-1}}{dr_{n-1}} \times \frac{dr_{n-1}}{dr_n} = -\frac{2\mathcal{V}_{n-1} \sin \varphi_{n-1}}{\mathbf{r} \cos^2 \varphi_{n-1}} \times \frac{dr_{n-1}}{dr_n}.$$

Note that $|dr_n| = \|dx_n\|/\sqrt{1+\mathcal{V}_n^2} \asymp \|dx_n\|$; hence $|dr_{n-1}/dr_n| \asymp \|dx_{n-1}\|/\|dx_n\|$, which is uniformly bounded due to uniform hyperbolicity (3.14). The factor $\cos^2 \varphi_{n-1}$ in the denominator is absorbed by $[1 + \tau_{n-1}\mathcal{B}_{n-1}^+]^2$ due to (3.12); thus

$$\frac{1}{[1 + \tau_{n-1}\mathcal{B}_{n-1}^+]^2} \left| \frac{d\mathcal{R}_{n-1}}{dr_n} \right| \leq \text{const.}$$

If x_{n-1} is of type N2, then we represent $|dr_{n-1}/dr_n|$ as

$$\left| \frac{dr_{n-1}}{dr_n} \right| = \frac{\|dx_{n-1}\|_p}{\|dx_n\|_p} \times \frac{\cos \varphi_n}{\cos \varphi_{n-1}} = \frac{\theta_n w_n}{w_{n-1}}$$

where

$$\theta_n = |1 + \tau_n \mathcal{B}_n^+|^{-1} = \|dx_n\|_p / \|dx_{n+1}\|_p$$

and

$$w_n = \theta_n^{-1} \cos \varphi_n = |1 + \tau_n \mathcal{B}_n^+| \cos \varphi_n.$$

Observe that $\theta_n \leq \Lambda^{-1} < 1$ and w_n is bounded above and below due to (3.12), i.e.

$$0 < w_{\min} \leq w_n \leq w_{\max} < \infty.$$

Combining these estimates with (4.5) gives

$$(4.7) \quad \left| \frac{d\mathcal{B}_n^-}{dr_n} \right| \leq C'' + \theta_{n-1}^2 \theta_n \frac{w_n}{w_{n-1}} \left| \frac{d\mathcal{B}_{n-1}^-}{dr_{n-1}} \right|$$

where $C'' = C''(\mathcal{D}) > 0$ is a constant. A simple recursive application of (4.7) gives

$$\left| \frac{d\mathcal{B}_n^-}{dr_n} \right| \leq \frac{w_{\max}}{w_{\min}} \left(\frac{C''}{1 - \Lambda^{-3}} + \Lambda^{-3n+1} \theta_0 \left| \frac{d\mathcal{B}^-}{dr} \right| \right).$$

Note that due to (4.4) and (3.12) we have $\sup_W \theta_0 |d\mathcal{B}^-/dr| < \infty$, so (4.3) is proved.

It remains to treat type N3 series of collisions. If x_{n-1} is of type N3, then

$$\left(\frac{\|dx_{n-1}\|_p}{\|dx_n\|_p} \right)^2 \frac{d\mathcal{B}_{n-1}^-}{dr_n} = \theta_{n-1}^3 \frac{\cos \varphi_n}{\cos \varphi_{n-1}} \frac{d\mathcal{B}_{n-1}^-}{dr_{n-1}},$$

thus

$$\frac{d\mathcal{B}_n^-}{dr_n} \leq C' + \theta_{n-1}^3 \frac{\cos \varphi_n}{\cos \varphi_{n-1}} \frac{d\mathcal{B}_{n-1}^-}{dr_{n-1}}$$

A simple recursive application of above formula gives

$$\begin{aligned} \left| \frac{d\mathcal{B}_n^-}{dr_n} \right| &\leq C' C (1 + \Lambda^{-2} + \Lambda^{-4} + \dots + \Lambda^{-2n}) + C^2 \Lambda^{-2n} \cos \varphi \frac{d\mathcal{B}}{dr} \\ &\leq C'' (1 - \Lambda^{-2})^{-1} + C^2 \Lambda^{-2n} \cos \varphi \frac{d\mathcal{B}}{dr}. \end{aligned}$$

Lastly, note that due to (4.4) and (3.12) we have $\sup_W \cos \varphi |d\mathcal{B}^-/dr| < \infty$, which completes the proof of Proposition 4.1. \square

We remark that due to the time reversibility, stable curves all have similar (dual) properties.

Next, we describe singularities for the map \mathcal{F}_\diamond . Put $\hat{\mathcal{S}}_0 = \partial\mathcal{M}_\diamond$ and denote by $\hat{\mathcal{S}}_n$ the singularities of the map \mathcal{F}_\diamond^n . Singularity curves for the map \mathcal{F}_\diamond are stable and those for $\mathcal{F}_\diamond^{-1}$ are unstable. It is easy to check directly that these curves have uniformly bounded curvature (some of them are actually straight lines). Thus all the curves in $\hat{\mathcal{S}}_n \setminus \hat{\mathcal{S}}_0$ for $n \geq 1$ are stable and have uniformly bounded curvature, and all the curves in $\hat{\mathcal{S}}_{-n} \setminus \hat{\mathcal{S}}_0$ for $n \geq 1$ are unstable and also have uniformly bounded curvature.

It is easy to see that singularities of the map \mathcal{F}_\diamond have the same general properties as they do in dispersing billiards [CM, Chapter 4]. In particular, the alignment of singularity lines takes place, i.e. the angle between the singularity lines of \mathcal{F}_\diamond^n (or $\mathcal{F}_\diamond^{-n}$) and stable (resp., unstable) manifolds converges to zero as $n \rightarrow \infty$. Also, the continuation of singularity lines holds, i.e. every singularity curve of \mathcal{F}_\diamond^n terminates either on another singularity curve or on $\partial\mathcal{M}_\diamond$. The singularity curves of $\hat{\mathcal{S}}_{-n} \cup \hat{\mathcal{S}}_m$ for any $m, n > 0$ divide \mathcal{M}_\diamond into curvilinear polygons whose internal angles do not exceed π (the ‘‘convexity’’).

Note that the sets $\hat{\mathcal{S}}_\infty$ and $\hat{\mathcal{S}}_{-\infty}$ are dense in \mathcal{M}_\diamond due to the hyperbolicity of the map \mathcal{F}_\diamond . This fact will be used to construct stable and unstable manifolds in the next section.

5 Stable and unstable manifolds

The properties of singularity curves described in the previous section allow us to construct stable and unstable manifolds for both stadia.

Let $x \in \mathcal{M}_\diamond \setminus \hat{\mathcal{S}}_{-\infty}$ and for any $n \geq 1$ denote by $\mathcal{Q}_{-n}(x)$ the connected component of the open set $\mathcal{M}_\diamond \setminus \hat{\mathcal{S}}_{-n}$ that contains x . The intersection of their closures

$$\tilde{W}^u(x) := \bigcap_{n=1}^{\infty} \overline{\mathcal{Q}_{-n}(x)}$$

is a closed continuous monotonically increasing curve. The unstable manifold $W^u(x)$ is the curve $\tilde{W}^u(x)$ without its endpoints. Its slope at every point $y \in W^u(x)$ equals $\mathcal{V}^u(y) = \mathcal{K} + \mathcal{B}^{u-}(y) \cos \varphi$, where the continued fraction

representing $\mathcal{B}^{u^-}(y)$ has the form

$$(5.1) \quad \frac{1}{|t^-(y)| + \frac{1}{\mathcal{R}_{-1} + \frac{1}{\tau_{-2} + \frac{1}{\mathcal{R}_{-2} + \frac{1}{\tau_{-3} + \frac{1}{\ddots}}}}}}.$$

where $t^-(y)$ is the time of the most recent collision in the past. The map $\mathcal{F}_\diamond^{-n}$ is smooth on $W^u(x)$ for all $n \geq 1$, and the preimages of $W^u(x)$ contract under $\mathcal{F}_\diamond^{-1}$ uniformly and exponentially in time. Proposition 4.1 ensures that unstable manifolds are C^2 smooth and have uniformly bounded derivatives. Stable manifolds $W^s(x)$ for $x \in \mathcal{M}_\diamond$ are constructed likewise and have similar (dual) properties.

Next we discuss the size of unstable manifolds. A point $x \in \mathcal{M}_\diamond$ divides $W^u(x)$ into two segments, and we denote by $r^u(x)$ the length (in the Euclidean metric) of the shorter one. If $W^u(x)$ is empty, then we put $r^u(x) = 0$.

Theorem 5.1. *$W^u(x)$ exists (i.e. $r^u(x) > 0$) for almost every $x \in \mathcal{M}_\diamond$. Furthermore,*

$$(5.2) \quad \mu_\diamond\{x \in \mathcal{M}_\diamond : r^u(x) < \varepsilon\} \leq C\varepsilon$$

for some constant $C = C(\mathcal{D}) > 0$ and all $\varepsilon > 0$.

Proof. For every point $x \in \mathcal{M}_\diamond$, denote by $d^u(x; \hat{\mathcal{S}}_1)$ the length of the shortest unstable curve that connects x with the set $\hat{\mathcal{S}}_1$.

First, we define a piecewise constant function $E(x)$ on \mathcal{M}_\diamond as follows: at a first sliding collision in a series of length k we set $E(x) = k$ and at a last collision in that series we set $E(x) = \sqrt{k}$; at a collision before a long series of k diametrical reflections at the large arc set $E(x) = k$; at a collision before a long series of k reflections at the flat sides $E(x) = k$. It follows from Section 3 that there exists $c > 0$, such that for any v at x

$$\|D_x \mathcal{F}_\diamond v\| \geq cE(x)\|v\|.$$

Furthermore, since $\mathcal{F}_\diamond: \mathcal{M}_\diamond \mapsto \mathcal{M}_\diamond$ is uniformly hyperbolic, there exist $\bar{c} > 0$ and $\Lambda > 1$, such that for any $x \in \mathcal{M}_\diamond$ and any unstable vector v at x

$$\|D_x \mathcal{F}_\diamond^n v\| \geq \bar{c} \Lambda^n \|v\|.$$

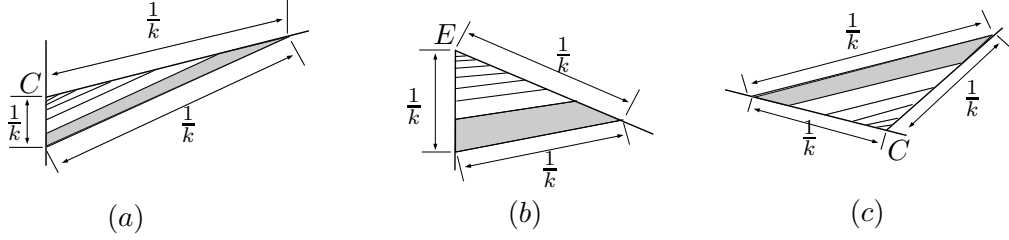


Figure 7: Singularity curves: (a) type N1, (b) type N2, (c) type N3.

Thus one can show that

$$r^u(x) \geq \min_{m \geq 1} cE(\mathcal{F}_\diamond^{-m}x) \bar{c} \Lambda^{m-1} d^u(\mathcal{F}_\diamond^{-m}x, \hat{\mathcal{S}}_1).$$

Choose any $\hat{\Lambda} \in (1, \Lambda)$, and define

$$r^*(x) = \min_{m \geq 1} cE(\mathcal{F}_\diamond^{-m}x) \bar{c} \hat{\Lambda}^{m-1} d^u(\mathcal{F}_\diamond^{-m}x, \hat{\mathcal{S}}_1).$$

Clearly, $r^u(x) \geq r^*(x)$. Denote

$$\tilde{\mathcal{U}}_\varepsilon^u(\hat{\mathcal{S}}_1) = \{x \in \mathcal{M}_\diamond : E(x) d^u(x, \hat{\mathcal{S}}_1) < \varepsilon\}$$

Next we will prove that

$$(5.3) \quad \mu_\diamond(\tilde{\mathcal{U}}_\varepsilon^u(\hat{\mathcal{S}}_1)) < C\varepsilon,$$

which requires a detailed analysis of singularities in the vicinities of the points where the singularity lines accumulate, i.e. the points E, B, C, D in the hexagon shown in Fig. 4. A close-up of the vicinities of points E and C is shown in Fig. 7; the picture near points B and D is symmetric. Points of first collisions in long series of k non-essential collisions (of type N1, N2 and N3) fill a grey quadrilateral near E (or C). All gray quadrilateral have dimensions $k^{-1} \times k^{-2}$.

The straight stadium has collisions of type N1 and N2 only. The intersection of $\tilde{\mathcal{U}}_\varepsilon^u$ with the quadrilateral in (a) lies within the $(ck^{-1/2}\varepsilon)$ -neighborhood of its boundary, and the intersection of $\tilde{\mathcal{U}}_\varepsilon^u$ with the quadrilateral in (b) lies within the $(ck^{-1}\varepsilon)$ -neighborhood of its boundary, where $c > 0$ is a constant. Now

$$(5.4) \quad \mu_\diamond(\tilde{\mathcal{U}}_\varepsilon^u(\hat{\mathcal{S}}_1)) < c \sum_k k^{-5/2}\varepsilon + c \sum_k k^{-2}\varepsilon < C\varepsilon$$

for some constants $c, C > 0$ (note that the extra factor k^{-1} is included here due to the density $\cos \varphi \asymp 1/k$ of the measure μ_\diamond). The drive-belt table has collisions of type N2 and N3 only, but the proof of (5.3) follows the same lines. Denote

$$D_n = \mathcal{F}_\diamond^n(\tilde{\mathcal{U}}_{c\hat{\Lambda}^{-n}}^u(\hat{\mathcal{S}}_1)) = \{x \in \mathcal{M}_\diamond : E(\mathcal{F}_\diamond^{-n}x)d^u(\mathcal{F}_\diamond^{-n}(x), \hat{\mathcal{S}}_1) < c\hat{\Lambda}^{-n}\}.$$

Then by the invariance of the measure μ_\diamond and (5.3)

$$\mu_\diamond(D_n) = \mu_\diamond(\tilde{\mathcal{U}}_{c\hat{\Lambda}^{-n}}^u(\hat{\mathcal{S}}_1)) \leq C\hat{\Lambda}^{-n}.$$

By the Borel-Cantelli lemma, the set $B = \bigcap_{m=1}^\infty \bigcup_{n \geq m} D_n$ has zero measure, i.e. $\mu_\diamond(B) = 0$. On the other hand, B consists of points $x \in \mathcal{M}_\diamond$, such that $r^*(x) = 0$. Thus for μ_\diamond -almost every $x \in \mathcal{M}_\diamond$, $r^*(x) \neq 0$. To prove (5.2), it is enough to show that

$$\mu_\diamond(x \in \mathcal{M}_\diamond : r^*(x) < \varepsilon) < C\varepsilon.$$

Notice that

$$\{x \in \mathcal{M}_\diamond : r^*(x) < \varepsilon\} = \bigcup_{m=1}^\infty \tilde{\mathcal{U}}_{(c\hat{\Lambda})^{-1}\hat{\Lambda}^{-m}\varepsilon}^u(\hat{\mathcal{S}}_1),$$

now (5.3) implies the result. \square

Remark 5.2. *We can prove a linear tail bound similar to (5.2) for the p -metric:*

$$\mu_\diamond\{x \in \mathcal{M}_\diamond : p^u(x) < \varepsilon\} \leq C\varepsilon$$

where $p^u(x)$ is the distance in the p -metric from x to the nearer endpoint of $W^u(x)$.

In fact we can define the function $E(x)$ as above. Then put

$$\tilde{\mathcal{U}}_{p,\varepsilon}^u(\hat{\mathcal{S}}_1) = \{x \in \mathcal{M}_\diamond : E(x) d_p^u(x, \hat{\mathcal{S}}_1) < \varepsilon\}$$

where $d_p^u(x, \hat{\mathcal{S}}_1)$ denotes the length (in the p-metric) of the shortest unstable curve that connects x with the set $\hat{\mathcal{S}}_1$. Lastly we show that $\mu_\diamond(\tilde{\mathcal{U}}_{p,\varepsilon}^u(\hat{\mathcal{S}}_1)) < C\varepsilon$. Note that (5.4) needs to be modified only slightly:

$$\mu_\diamond(\tilde{\mathcal{U}}_{p,\varepsilon}^u(\hat{\mathcal{S}}_1)) < c \sum_k k^{-3/2} \varepsilon + c \sum_k k^{-2} \varepsilon < C\varepsilon.$$

Lemma 5.3. *Let $W \subset \mathcal{M}_\diamond$ be an unstable curve on which \mathcal{F}_\diamond is smooth. Then $|\mathcal{F}_\diamond(W)| \leq C\sqrt{|W|}$, where $C = C(\mathcal{D}) > 0$ is a constant and $|W|$ denotes the Euclidean length of W .*

Proof. We denote by $x = (r, \varphi)$ points on the curve W and by $x_1 = (r_1, \varphi_1)$ points on its image $\mathcal{F}_\diamond(W)$. The claim is trivial unless τ is large or $\cos \varphi_1 \approx 0$ (cf. (3.15)). If τ is large, then the unstable curve W must ‘squeeze’ between two singularity lines which are $\sim 1/\tau^2$ apart, cf. the end of Section 2, hence $|W| = \mathcal{O}(\tau^2)$, hence $|\mathcal{F}_\diamond(W)| = \mathcal{O}(\tau|W|) = \mathcal{O}(\sqrt{|W|})$. If $\cos \varphi_1 \approx 0$, there are two cases to consider. First, if W consists of first collisions in a long series of k sliding collisions, then $|W| \leq \text{const} \cdot k^{-2}$; hence

$$|\mathcal{F}_\diamond(W)| \asymp k|W| \leq \text{const} \cdot |W|^{1/2}.$$

The more difficult case is where W consists of last collisions in a long series of k sliding collisions. Then $\mathcal{F}_\diamond(W)$ consists of *first* collisions of the next sliding series (on the opposite arc); thus $\|dx_1\| \asymp dr_1 \asymp d\varphi_1$ on $\mathcal{F}_\diamond(W)$. We introduce a new variable $s = \cos \varphi_1$ on $\mathcal{F}_\diamond(W)$ and denote by s_{\min} and s_{\max} its extreme values on that curve. Then $\|dx_1\| \asymp ds$ on $\mathcal{F}_\diamond(W)$ and $|\mathcal{F}_\diamond(W)| \asymp s_{\max} - s_{\min}$. Denote by $\|dx_1\|/\|dx\| \asymp s$ the (local) factor of contraction of the curve $\mathcal{F}_\diamond(W)$ under the map $\mathcal{F}_\diamond^{-1}$; cf. (3.15). Now

$$|W| = \int_W \|dx\| \asymp \int_{\mathcal{F}_\diamond(W)} s \|dx_1\| \asymp \int_{s_{\min}}^{s_{\max}} s ds \asymp s_{\max}^2 - s_{\min}^2.$$

Now the lemma follows from the obvious: $(s_{\max} - s_{\min})^2 \leq s_{\max}^2 - s_{\min}^2$. \square

Remark 5.4. *Observe that if a sequence of unstable manifolds $\{W_i^u\}$ converges, as $i \rightarrow \infty$, to a curve W (in the C^0 metric), then W (taken without its endpoints) is an unstable manifold itself. Furthermore, for μ_\diamond -almost every $x \in \mathcal{M}_\diamond$ both endpoints of $W^u(x)$ belong to $\hat{\mathcal{S}}_{-\infty}$.*

We have constructed and described stable and unstable manifolds for the return map $\mathcal{F}_\diamond: \mathcal{M}_\diamond \rightarrow \mathcal{M}_\diamond$. Of course, they coincide with stable and unstable manifolds for the original map \mathcal{F} on \mathcal{M}_\diamond as well. By iterating them under the map \mathcal{F} into the area $\mathcal{M} \setminus \mathcal{M}_\diamond$ we readily obtain stable and unstable manifolds for the map \mathcal{F} in the entire collision space \mathcal{M} .

6 u-SRB densities and distortion bounds

In the previous section we constructed the maximal unstable manifold $W^u(x)$ for almost every point $x \in \mathcal{M}_\diamond$. We note that $W^u(x)$ does not include its end points, hence for any $x, y \in \mathcal{M}_\diamond$ the manifolds $W^u(x)$ and $W^u(y)$ either coincide or are disjoint. Let ξ^u denote the partition of \mathcal{M}_\diamond into maximal unstable manifolds. Precisely, for every point $x \in \mathcal{M}_\diamond$ we put $\xi_x^u = W^u(x)$, if the latter is not empty, and $\xi_x^u = \{x\}$ otherwise. Note that if y is an endpoint of $W^u(x)$, then $W^u(y) = \emptyset$, hence $\xi_y^u = \{y\}$. Similarly, we can define ξ^s . Both partitions are measurable, see [CM, Section 5.1], hence the invariant measure μ induces conditional (probability) measure, $\nu_{W^u(x)}$ (or $\nu_{W^s(x)}$), on a.e. $W^u(x)$ (or $W^s(x)$), see necessary definitions and facts about measurable partitions and conditional distributions in [CM, Appendix A].

It is standard [CM, Section 5.2] that $\nu_{W^u(x)}$ are absolutely continuous and their densities ρ_W (u-SRB densities) satisfy a fundamental formula:

$$(6.1) \quad \frac{\rho_W(y)}{\rho_W(z)} = \lim_{n \rightarrow \infty} \frac{\mathcal{J}_W \mathcal{F}_\diamond^{-n}(y)}{\mathcal{J}_W \mathcal{F}_\diamond^{-n}(z)}$$

for all $y, z \in W$. Here $\mathcal{J}_W \mathcal{F}_\diamond^{-n}(x) = \|D_x \mathcal{F}_\diamond^{-n} w\| / \|w\|$, where w is a nonzero tangent vector to W at the point x .

Proposition 6.1. *Let $r^*(x) > 0$ (in the notation of the previous section). Then the limit (6.1) is finite for all $y, z \in W^u(x)$, hence $\rho_{W^u(x)}$ exists.*

Proof. First, taking the logarithm and using the chain rule reduce this problem to the convergence of the series

$$(6.2) \quad \sum_{n=0}^{\infty} \left(\ln \mathcal{J}_{W_n} \mathcal{F}_\diamond^{-1}(y_n) - \ln \mathcal{J}_{W_n} \mathcal{F}_\diamond^{-1}(z_n) \right),$$

where $W_n = \mathcal{F}_\diamond^{-n}(W)$ and $y_n = \mathcal{F}_\diamond^{-n}(y)$ (the same for z_n). We pick $x \in W$ and denote $x_n = \mathcal{F}_\diamond^{-n}(x)$, $\tau_n = \tau(x_n)$, and $\mathcal{B}_n, \mathcal{K}_n$, etc. are taken at the point

x_n . Then

$$\mathcal{J}_{W_n} \mathcal{F}_{\diamond}^{-1}(x_n) = \frac{\|dx_{n+1}\|}{\|dx_n\|} = \frac{1}{|1 + \tau_{n+1} \mathcal{B}_{n+1}^+|} \frac{\cos \varphi_n}{\cos \varphi_{n+1}} \frac{\sqrt{1 + \mathcal{V}_{n+1}^2}}{\sqrt{1 + \mathcal{V}_n^2}}$$

Therefore

$$(6.3) \quad \begin{aligned} \ln \mathcal{J}_{W_n} \mathcal{F}_{\diamond}^{-1}(x_n) &= \ln \cos \varphi_n - \ln \cos \varphi_{n+1} + \frac{1}{2} \ln(1 + \mathcal{V}_{n+1}^2) - \frac{1}{2} \ln(1 + \mathcal{V}_n^2) \\ &\quad - \ln|1 + \tau_{n+1} \mathcal{B}_{n+1}^+|. \end{aligned}$$

And again, due to the uniform hyperbolicity of \mathcal{F}_{\diamond} , $\text{dist}(y_n, z_n) \leq \text{diam}(W_n) \leq \hat{C} \Lambda^{-n}$. We obtain

$$|\ln \mathcal{J}_{W_n} \mathcal{F}_{\diamond}^{-1}(y_n) - \ln \mathcal{J}_{W_n} \mathcal{F}_{\diamond}^{-1}(z_n)| \leq \hat{C} \Lambda^{-n} \max \left| \frac{d}{dx_n} \ln \mathcal{J}_{W_n} \mathcal{F}_{\diamond}^{-1}(x_n) \right|$$

where the maximum is taken over all $x_n \in W_n$ and d/dx_n denotes the derivative with respect to the Euclidean length on W_n .

Next we differentiate (6.3) with respect to x_n . Observe, however, that (6.3) contains functions that depend on x_{n+1} , but those can be handled by the chain rule

$$\frac{d}{dx_n} = \frac{dx_{n+1}}{dx_n} \frac{d}{dx_{n+1}} = \mathcal{J}_{W_n} \mathcal{F}_{\diamond}^{-1}(x_n) \frac{d}{dx_{n+1}}$$

(note also that the factor $\mathcal{J}_{W_n} \mathcal{F}_{\diamond}^{-1}(x_n)$ is uniformly bounded.) Our results in the previous section imply that the quantities $\tau, \varphi, \mathcal{B}^-$ and \mathcal{V} are C^1 smooth functions on unstable manifolds, with uniformly bounded derivatives. Also, all the expressions on the right-hand side of (6.3), except the first and last logarithmic terms, are uniformly bounded (since $\cos \varphi$ may be small and the free path τ is not bounded from above).

Applying Lemma 3.1 to the last collision x_n of a series of collisions at the same arc and noticing that $|1 + \tau_{n+1} \mathcal{B}_{n+1}^+| = |1 - \tau_{n+1} \mathcal{B}_n^-|^{-1}$ we obtain

$$(6.4) \quad \begin{aligned} \frac{d}{dx_n} \ln|1 - \tau_{n+1} \mathcal{B}_n^-| &= \frac{\left| \frac{d\tau_{n+1}}{dx_n} \mathcal{B}_n^- + \tau_n \frac{d\mathcal{B}_n^-}{dx_n} \right|}{|1 - \tau_{n+1} \mathcal{B}_n^-|} \\ &= \frac{\|dx_{n+1}\|_p}{\|dx_n\|_p} \left| \frac{d\tau_{n+1}}{dx_n} \mathcal{B}_n^- + \tau_n \frac{d\mathcal{B}_n^-}{dx_n} \right|. \end{aligned}$$

By our results in Section 3, we know that

$$\frac{\|dx_{n+1}\|_p}{\|dx_n\|_p} \leq \frac{1}{2kr} < \frac{1}{2kr \cos \varphi_n} = \frac{1}{\tau_n},$$

thus we arrive at

$$(6.5) \quad \frac{d}{dx_n} \ln \mathcal{J}_{W_n} \mathcal{F}_{\diamond}^{-1}(x_n) = P_n(x_n) + \frac{|\mathcal{V}_n|}{\cos \varphi_n} Q_n(x_n)$$

where P_n and Q_n are uniformly bounded functions of x_n . Now

$$(6.6) \quad |\ln \mathcal{J}_{W_n} \mathcal{F}_{\diamond}^{-1}(y_n) - \ln \mathcal{J}_{W_n} \mathcal{F}_{\diamond}^{-1}(z_n)| \leq \frac{\text{const} \cdot \Lambda^{-n}}{\min_x \cos \varphi_n}$$

where the minimum is taken over all $x \in W$.

To deal with the potentially small denominator here, we use our assumption that $r^*(x) > 0$ for some point $x \in W$ (and hence, for all points $x \in W$, see the proof of Proposition 5.9). We also restrict our analysis to the segment $W[y; z] \subset W$ of the curve W with endpoints y and z . Then we have $d^u(\mathcal{F}^{-n}x, \mathcal{S}_1) \geq \hat{\Lambda}^{-n}$, hence $\cos \varphi_n > c\hat{\Lambda}^{-n}$ for all $n \geq 1$ and all $x \in W[y, z]$ with some $c = c(y, z) > 0$. We also recall that $\hat{\Lambda} < \Lambda$, hence

$$\min_x \cos \varphi_n > \frac{1}{2} c \hat{\Lambda}^{-n}.$$

Thus (6.2) converges exponentially, and the u-SRB density ρ_W exists. \square

Next we derive distortion bounds. Let W be an unstable curve such that $W_n = \mathcal{F}_{\diamond}^{-n}(W)$ is also an unstable curve for all $0 \leq n \leq N - 1$. In addition, we assume that $W \cap \hat{\mathcal{S}}_1 = \emptyset$. For every point $x \in W$ we put $x_n = \mathcal{F}_{\diamond}^{-n}(x)$ and denote by $\mathcal{J}_W \mathcal{F}_{\diamond}^{-n}(x)$ the factor of contraction of W under the map $\mathcal{F}_{\diamond}^{-n}$ at x . The following holds:

Lemma 6.2. *For every $y, z \in W$ and every $1 \leq n \leq N$ we have*

$$C_d^{-1} \leq e^{-C|W|^{1/2}} \leq \frac{\mathcal{J}_W \mathcal{F}_{\diamond}^{-n}(y)}{\mathcal{J}_W \mathcal{F}_{\diamond}^{-n}(z)} \leq e^{C|W|^{1/2}} \leq C_d,$$

where $C = C(\mathcal{D}) > 0$ and $C_d = C_d(\mathcal{D}) > 0$ are constants.

Proof. Taking the logarithm and using the chain rule give

$$\begin{aligned}
|\ln \mathcal{J}_W \mathcal{F}_\diamond^{-n}(y) - \ln \mathcal{J}_W \mathcal{F}_\diamond^{-n}(z)| &\leq \sum_{i=0}^{n-1} |\ln \mathcal{J}_{W_i} \mathcal{F}_\diamond^{-1}(y_i) - \ln \mathcal{J}_{W_i} \mathcal{F}_\diamond^{-1}(z_i)| \\
&\leq \sum_{i=0}^{n-1} |W_i| \max \left| \frac{d}{dx_i} \ln \mathcal{J}_{W_i} \mathcal{F}_\diamond^{-1}(x_i) \right| \\
&\leq \text{const} \sum_{i=0}^{n-1} |W_i| (1 + |\mathcal{V}_i| / \cos \varphi_i)
\end{aligned}$$

where at the last step we used (6.5). Now we claim that

$$(6.7) \quad |W_i| |\mathcal{V}_i| / \cos \varphi_i \leq \text{const} |W_i|^{1/2}.$$

This is trivial unless $\cos \varphi_i$ is small, which happens only at first and last collisions in long series of sliding collisions. At a first sliding collision $|W_i| = \mathcal{O}(k^{-2})$, and $\cos \varphi_i \asymp k^{-1}$ and $|\mathcal{V}_i| \asymp 1$ (here k is the number of collisions in the series), which implies (6.7). At a last sliding collision $|W_i| \asymp k^{-1}$ and $\cos \varphi_i \asymp k^{-1}$, but we also have $|\mathcal{V}_i| \asymp k^{-1}$ (see Table 1), which completes the proof of (6.7). Hence

$$\begin{aligned}
|\ln \mathcal{J}_W \mathcal{F}_\diamond^{-n}(y) - \ln \mathcal{J}_W \mathcal{F}_\diamond^{-n}(z)| &\leq \text{const} \sum_{i=0}^{n-1} |W_i|^{1/2} \\
&\leq \text{const} |W|^{1/2},
\end{aligned}$$

where at the last step we used the uniform hyperbolicity of \mathcal{F}_\diamond . Now Lemma 6.2 is proved. \square

Corollary 6.3. *For every $x \in W$ and every $1 \leq n \leq N$*

$$C_d^{-1} \leq \frac{\mathcal{J}_W \mathcal{F}_\diamond^{-n}(x)}{|W_n|/|W|} \leq C_d.$$

We remark that in dispersing billiards, in order to ensure distortion bounds one needs to subdivide the collision space into countable many homogeneity strips [CM, Section 5.3]. Here we do not need those – our distortion bounds hold for all unstable curves, provided they do not intersect $\hat{\mathcal{S}}_1$. The reason is that the singularity lines of $\hat{\mathcal{S}}_1$ already divide the ‘hazardous’ area where $\cos \varphi \approx 0$ into sufficiently narrow strips (see Fig. 7), which ensures the homogeneity of unstable curves in each strip.

Theorem 6.4 (Distortion bounds). *For every unstable manifold $W \subset \mathcal{M}_\diamond$ that does not intersect $\hat{\mathcal{S}}_1$*

$$\left| \frac{d}{dx} \ln \rho_W(x) \right| \leq \frac{C}{|W|^{1/2}},$$

where $C = C(\mathcal{D}) > 0$ is a constant.

Proof. We fix a point $\bar{x} \in W$. Then due to (6.1) and the chain rule

$$\ln \rho_W(x) = \ln \rho_W(\bar{x}) + \sum_{n=0}^{\infty} (\ln \mathcal{J}_{W_n} \mathcal{F}_\diamond^{-1}(x_n) - \ln \mathcal{J}_{W_n} \mathcal{F}_\diamond^{-1}(\bar{x}_n));$$

hence

$$\begin{aligned} \frac{d}{dx} \ln \rho_W(x) &= \sum_{n=0}^{\infty} \frac{d}{dx} \ln \mathcal{J}_{W_n} \mathcal{F}_\diamond^{-1}(x_n) \\ &= \sum_{n=0}^{\infty} \frac{dx_n}{dx} \frac{d}{dx_n} \ln \mathcal{J}_{W_n} \mathcal{F}_\diamond^{-1}(x_n) \\ &= \sum_{n=0}^{\infty} \mathcal{J}_W \mathcal{F}_\diamond^{-n}(x) \left[P_n(x_n) + \frac{|\mathcal{V}_n| Q_n(x_n)}{\cos \varphi_n} \right], \end{aligned}$$

where P_n and Q_n are uniformly bounded functions of x_n from (6.5). Therefore,

$$\begin{aligned} \left| \frac{d}{dx} \ln \rho_W(x) \right| &\leq \text{const} \sum_{n=0}^{\infty} \mathcal{J}_W \mathcal{F}_\diamond^{-n}(x) [1 + \mathcal{V}_n / \cos \varphi_n] \\ &\leq \text{const} \sum_{n=0}^{\infty} \frac{|W_n| / |W|}{|W_n|^{1/2}} \\ &\leq \text{const} \sum_{n=0}^{\infty} \frac{\Lambda^{-n/2}}{|W|^{1/2}} \end{aligned}$$

where we used (6.7), Corollary 6.3, and the uniform hyperbolicity of \mathcal{F}_\diamond ; cf. (3.14). Theorem 6.4 is proved. \square

Corollary 6.5. *For every $x, y \in W$*

$$C_d^{-1} \leq e^{-C|W|^{1/2}} \leq \frac{\rho_W(x)}{\rho_W(y)} \leq e^{C|W|^{1/2}} \leq C_d,$$

where $C = C(\mathcal{D}) > 0$ is a constant.

Thus we derived all the basic distortion bounds for both stadia. We will not estimate higher order derivatives here to avoid unnecessary complications.

7 Absolute continuity

Here we estimate the Jacobian of the holonomy map. Let $W^1, W^2 \subset \mathcal{M}_\diamond$ be two unstable curves. Denote

$$W_*^i = \{x \in W^i : W^s(x) \cap W^{3-i} \neq \emptyset\}$$

for $i = 1, 2$. The holonomy map $\mathbf{h}: W_*^1 \rightarrow W_*^2$ takes points $x \in W_*^1$ to $\bar{x} = W^s(x) \cap W^2$. The Jacobian of \mathbf{h} , with respect to the Lebesgue measures on W^1 and W^2 , satisfies a basic formula:

$$(7.1) \quad J\mathbf{h}(x) = \lim_{n \rightarrow \infty} \frac{\mathcal{J}_{W^1} \mathcal{F}_\diamond^n(x)}{\mathcal{J}_{W^2} \mathcal{F}_\diamond^n(\mathbf{h}(x))}.$$

While the general theory of hyperbolic maps [KS] guarantees that the Jacobian is positive and finite for almost every point $x \in W_*^1$, it is important to obtain explicit bounds on it.

We assume that W^1 and W^2 are C^2 smooth curves with uniformly bounded first and second derivatives (then their future images will have uniformly bounded derivatives as well, due to Proposition 4.1).

Let $x \in W_*^1$ and $\bar{x} = \mathbf{h}(x) \in W_*^2$. We assume that the segment of $W^s(x)$ between the points x and \bar{x} does not cross $\hat{\mathcal{S}}_{-1}$ (in the case of dispersing billiards, a stronger assumption – that of homogeneity of $W^s(x)$ – must be made [CM, Chapter 5]). We put $\delta = \text{dist}(x, \bar{x})$ and denote by $\gamma = |\mathcal{V}(x) - \mathcal{V}(\bar{x})|$ the ‘angle’ between the tangent vectors to the curves W^1 and W^2 at the points x and \bar{x} , respectively.

Theorem 7.1. *The Jacobian of the holonomy map \mathbf{h} is uniformly bounded*

$$C^{-1} \leq J\mathbf{h}(x) \leq C,$$

for all $x \in W_*^1$; here $C = C(\mathcal{D}) > 1$ is a constant. Moreover,

$$(7.2) \quad A^{-\gamma - \delta^{1/2}} \leq J\mathbf{h}(x) \leq A^{\gamma + \delta^{1/2}},$$

where $A = A(\mathcal{D}) > 1$ is a constant.

Proof. Denote $W_n^i = \mathcal{F}_\diamond^n(W^i)$ for $i = 1, 2$ and $n \geq 1$. Also denote $x_n = \mathcal{F}_\diamond^n(x)$ and $\bar{x}_n = \mathcal{F}_\diamond^n(\bar{x})$ and put $\delta_n = \text{dist}(x_n, \bar{x}_n)$. Due to the uniform hyperbolicity of \mathcal{F}_\diamond (cf. (3.14)), $\delta_n \leq \hat{C}\delta\Lambda^{-n}$, where $\hat{C} = 1/\hat{c}$.

Taking the logarithm of (7.1) and using the chain rule give

$$(7.3) \quad \ln \mathcal{J}h(x) = \sum_{n=0}^{\infty} \left(\ln \mathcal{J}_{W_n^1} \mathcal{F}_\diamond(x_n) - \ln \mathcal{J}_{W_n^2} \mathcal{F}_\diamond(\bar{x}_n) \right).$$

Due to (3.13), (3.3), and (2.2)

$$\begin{aligned} \mathcal{J}_{W_n^1} \mathcal{F}_\diamond(x_n) &= |1 + \tau_n \mathcal{B}_n^+| \frac{\cos \varphi_n}{\cos \varphi_{n+1}} \frac{\sqrt{1 + \mathcal{V}_{n+1}^2}}{\sqrt{1 + \mathcal{V}_n^2}} \\ &= \frac{|\cos \varphi_n + \tau_n(\mathcal{K}_n + \mathcal{V}_n)|}{\cos \varphi_{n+1}} \frac{\sqrt{1 + \mathcal{V}_{n+1}^2}}{\sqrt{1 + \mathcal{V}_n^2}}, \end{aligned}$$

where, as usual, $\tau_n = \tau(x_n)$, and $\mathcal{B}_n, \mathcal{K}_n$, etc., are taken at the point x_n . Therefore

$$(7.4) \quad \begin{aligned} \ln \mathcal{J}_{W_n^1} \mathcal{F}_\diamond(x_n) &= -\ln \cos \varphi_{n+1} + \frac{1}{2} \ln(1 + \mathcal{V}_{n+1}^2) - \frac{1}{2} \ln(1 + \mathcal{V}_n^2) \\ &\quad + \ln |\cos \varphi_n + \tau_n(\mathcal{K}_n + \mathcal{V}_n)|. \end{aligned}$$

Using similar notation at \bar{x}_n we get

$$(7.5) \quad \begin{aligned} \ln \mathcal{J}_{W_n^2} \mathcal{F}_\diamond(\bar{x}_n) &= -\ln \cos \bar{\varphi}_{n+1} + \frac{1}{2} \ln(1 + \bar{\mathcal{V}}_{n+1}^2) - \frac{1}{2} \ln(1 + \bar{\mathcal{V}}_n^2) \\ &\quad + \ln |\cos \bar{\varphi}_n + \bar{\tau}_n(\mathcal{K}_n + \bar{\mathcal{V}}_n)|. \end{aligned}$$

(Note that \mathcal{K}_n is the same at both points x_n and \bar{x}_n .) Comparing the first terms of the above expressions gives

$$\begin{aligned} |\ln \cos \varphi_{n+1} - \ln \cos \bar{\varphi}_{n+1}| &\leq \frac{\text{const} |\varphi_{n+1} - \bar{\varphi}_{n+1}|}{\cos \varphi_{n+1}} \\ &\leq \text{const} \delta_{n+1}^{1/2} \end{aligned}$$

where we used (6.7), more precisely, its ‘time reversal’ counterpart. All the other terms in (7.4) and (7.5) are uniformly bounded and differentiable; thus it easily follows that

$$(7.6) \quad \left| \ln \mathcal{J}_{W_n^1} \mathcal{F}_\diamond(x_n) - \ln \mathcal{J}_{W_n^2} \mathcal{F}_\diamond(\bar{x}_n) \right| \leq C(\delta_{n+1}^{1/2} + \gamma_n + \gamma_{n+1} + \delta_n)$$

where $C > 0$ is a constant and $\gamma_n = |\Delta\mathcal{V}_n| = |\mathcal{V}_n - \bar{\mathcal{V}}_n|$ stands for the ‘angle’ between the tangent vectors to the curves W_n^1 and W_n^2 at the points x_n and \bar{x}_n , respectively (note that $\gamma_0 = \gamma$).

Due to Lemma 5.3 (more precisely, due to its ‘time reversal’ counterpart), we have $\delta_n \leq C\delta_{n+1}^{1/2}$; thus the term δ_n in (7.6) may be dropped. It remains to estimate γ_n for all $n \geq 0$. For brevity, we denote $\Delta\mathcal{B}_n^- = \mathcal{B}_n^- - \bar{\mathcal{B}}_n^-$, $\Delta\tau_n = \tau_n - \bar{\tau}_n$, etc. First we estimate $\Delta\mathcal{B}_{n+1}^-$ by using (3.4):

$$\begin{aligned}
\Delta\mathcal{B}_{n+1}^- &= \frac{1}{\tau_n + 1/\mathcal{B}_n^+} - \frac{1}{\bar{\tau}_n + 1/\bar{\mathcal{B}}_n^+} \\
&= -\frac{1}{\tau_n + 1/\mathcal{B}_n^+} \frac{1}{\bar{\tau}_n + 1/\bar{\mathcal{B}}_n^+} \left(\Delta\tau_n + \frac{1}{\mathcal{B}_n^+} - \frac{1}{\bar{\mathcal{B}}_n^+} \right) \\
(7.7) \quad &= -\frac{\Delta\tau_n}{(\tau_n + 1/\mathcal{B}_n^+)(\bar{\tau}_n + 1/\bar{\mathcal{B}}_n^+)} + \frac{\Delta\mathcal{R}_n + \Delta\mathcal{B}_n^-}{(1 + \tau_n\mathcal{B}_n^+)(1 + \bar{\tau}_n\bar{\mathcal{B}}_n^+)}
\end{aligned}$$

(recall that $\mathcal{B}_n^+ = \mathcal{R}_n + \mathcal{B}_n^-$).

Now the first term in (7.7) is bounded by

$$\text{const } \Delta\tau_n \leq \text{const}(\delta_n + \delta_{n+1}) \leq \text{const } \delta_n.$$

Next,

$$\frac{\Delta\mathcal{R}_n}{(1 + \tau_n\mathcal{B}_n^+)(1 + \bar{\tau}_n\bar{\mathcal{B}}_n^+)} \leq \frac{2\mathcal{K}_n \cos \bar{\varphi}_n - 2\mathcal{K}_n \cos \varphi_n}{(\cos \varphi_n + \tau_n(\mathcal{K}_n + \mathcal{V}_n))(\cos \bar{\varphi}_n + \bar{\tau}_n(\mathcal{K}_n + \bar{\mathcal{V}}_n))}.$$

Since the denominator is bounded away from zero, due to (3.12), the absolute value of the fraction is $\mathcal{O}(\delta_n)$; thus (7.7) reduces to

$$\Delta\mathcal{B}_{n+1}^- = \tilde{Q}_n^{(1)} + \frac{\Delta\mathcal{B}_n^-}{(1 + \tau_n\mathcal{B}_n^+)(1 + \bar{\tau}_n\bar{\mathcal{B}}_n^+)},$$

where $|\tilde{Q}_n^{(1)}| \leq \text{const } \delta_n$. Next, due to (2.2)

$$\begin{aligned}
\Delta\mathcal{V}_{n+1} &= \mathcal{B}_{n+1}^- \cos \varphi_{n+1} - \bar{\mathcal{B}}_{n+1}^- \cos \bar{\varphi}_{n+1} \\
&= \tilde{Q}_{n+1}^{(2)} + \cos \varphi_{n+1} \Delta\mathcal{B}_{n+1}^-,
\end{aligned}$$

where $|\tilde{Q}_{n+1}^{(2)}| \leq \text{const } \delta_{n+1}$. Combining the last two estimates gives

$$\Delta\mathcal{V}_{n+1} = \tilde{Q}_n^{(3)} + \frac{\cos \varphi_{n+1}}{\cos \varphi_n} \frac{\Delta\mathcal{V}_n}{(1 + \tau_n\mathcal{B}_n^+)(1 + \bar{\tau}_n\bar{\mathcal{B}}_n^+)},$$

where $|\tilde{Q}_n^{(3)}| \leq \text{const } \delta_n$. Now consider the fraction

$$u_n := \frac{\cos \varphi_{n+1}}{\cos \varphi_n (1 + \tau_n \mathcal{B}_n^+) (1 + \bar{\tau}_n \bar{\mathcal{B}}_n^+)}.$$

It is easy to verify that for all $0 \leq k \leq n$

$$|u_n u_{n-1} \cdots u_k| \leq C/\Lambda^{n-k}$$

where $C = C(\mathcal{D}) > 0$ is a constant, and

$$(7.8) \quad \begin{aligned} \gamma_n = |\Delta \mathcal{V}_n| &\leq \text{const} \left(\sum_{k=0}^n \delta_k / \Lambda^{n-k} + \gamma / \Lambda^n \right) \\ &\leq \text{const} \left(\delta n / \Lambda^n + \gamma / \Lambda^n \right). \end{aligned}$$

Combining (7.8) with (7.6) yields

$$(7.9) \quad \left| \ln \mathcal{J}_{W_n^1} \mathcal{F}_\diamond(x_n) - \ln \mathcal{J}_{W_n^2} \mathcal{F}_\diamond(\bar{x}_n) \right| \leq C \left(\frac{\delta^{1/2}}{\Lambda^{n/3}} + \frac{\delta n}{\Lambda^n} + \frac{\gamma}{\Lambda^n} \right),$$

where $C = C(\mathcal{D}) > 0$ is a constant. Summing up over n gives

$$|\ln \mathbf{J}\mathbf{h}(x)| \leq \text{const}(\gamma + \delta^{1/2}),$$

which completes the proof of the theorem. \square

The bound (7.2) can be improved to

$$A^{-\delta^{1/2}} \leq \mathbf{J}\mathbf{h}(x) \leq A^{\delta^{1/2}}$$

if the curves W^1 and W^2 do not intersect and extend beyond the points x and \bar{x} by at least the distance $D\delta^{1/2}$, where $D = D(\mathcal{D}) > 0$ is a large constant, see [CM].

Lastly we show that the Jacobian $\mathbf{J}\mathbf{h}(x)$, as a function of $x \in W_*^1$ is ‘dynamically Hölder continuous’. Let $\mathcal{Q}_n(x)$ again denote the open connected component of the set $\mathcal{M}_\diamond \setminus \hat{\mathcal{S}}_n$ containing the point x . For two points $x, y \in \mathcal{M}_\diamond$ denote by

$$(7.10) \quad \mathbf{s}_+(x, y) = \min\{n \geq 0 : y \notin \mathcal{Q}_n(x)\}$$

the ‘separation time’.

Proposition 7.2. *There are constants $C > 0$ and $\theta \in (0, 1)$ such that*

$$|\ln J\mathbf{h}(x) - \ln J\mathbf{h}(y)| \leq C\theta^{\mathbf{s}_+(x,y)}.$$

Proof. Denote $\bar{x} = \mathbf{h}(x)$ and $\bar{y} = \mathbf{h}(y)$. Observe that $\mathbf{s}_+(\bar{x}, \bar{y}) = \mathbf{s}_+(x, y)$; this follows from the continuation property of singularity lines (Section 4). Using the notation of (7.3) and the triangle inequality gives

$$\begin{aligned} \Delta: &= |\ln J\mathbf{h}(x) - \ln J\mathbf{h}(y)| \\ &\leq \sum_{n=0}^{\infty} |\ln \mathcal{J}_{W_n^1} \mathcal{F}_{\diamond}(x_n) - \ln \mathcal{J}_{W_n^2} \mathcal{F}_{\diamond}(\bar{x}_n) - \ln \mathcal{J}_{W_n^1} \mathcal{F}_{\diamond}(y_n) + \ln \mathcal{J}_{W_n^2} \mathcal{F}_{\diamond}(\bar{y}_n)|. \end{aligned}$$

Let $m = \mathbf{s}_+(x, y)/2$. Then we apply the estimate (7.9) to all $n > m$ and Lemma 6.2 (on distortion bounds) to all $n \leq m$. This proves our claim with $\theta = \Lambda^{-1/4}$. \square

Acknowledgement. We thank P. Bálint and R. Markarian for useful discussions and anonymous referees for many helpful remarks. N. Chernov was partially supported by NSF grant DMS-0354775. H.-K. Zhang was partially supported by SRF for ROCS, SEM.

References

- [BG] P. Bálint and S. Gouëzel, *Limit theorems in the stadium billiard*, Comm. Math. Phys. **263** (2006), 461–512.
- [BSC1] L. A. Bunimovich, Ya. G. Sinai, and N. I. Chernov, *Markov partitions for two-dimensional billiards*, Russ. Math. Surv. **45** (1990), 105–152.
- [BSC2] L. A. Bunimovich, Ya. G. Sinai, and N. I. Chernov, *Statistical properties of two-dimensional hyperbolic billiards*, Russ. Math. Surv. **46** (1991), 47–106.
- [B1] L. A. Bunimovich, *On billiards close to dispersing*, Math. USSR. Sb. **23** (1974), 45–67.
- [B2] L. A. Bunimovich, *The ergodic properties of certain billiards*, Funk. Anal. Prilozh. **8** (1974), 73–74.

- [B3] L. A. Bunimovich, *On ergodic properties of nowhere dispersing billiards*, Comm. Math. Phys. **65** (1979), 295–312.
- [B4] L. A. Bunimovich, *On absolutely focusing mirrors*, In *Ergodic Theory and related topics, III (Güstrow, 1990)*. Edited by U. Krengel et al., Lecture Notes in Math. **1514**, Springer, Berlin (1992), 62–82.
- [C1] N. Chernov, *Decay of correlations and dispersing billiards*, J. Stat. Phys. **94** (1999), 513–556.
- [C2] N. Chernov, *Sinai billiards under small external forces*, Ann. H. Poincaré **2** (2001), 197–236.
- [CM] N. Chernov and R. Markarian, *Chaotic Billiards*, Mathematical Surveys and Monographs, **127**, AMS, Providence, RI, 2006.
- [CZ1] N. Chernov and H.-K. Zhang, *Billiards with polynomial mixing rates*, Nonlinearity **18** (2005), 1527–1553.
- [CZ2] N. Chernov and H.-K. Zhang, *Optimal estimates for correlations in billiards*, Comm. Math. Phys. (to appear).
- [D] V. Donnay, *Using integrability to produce chaos: billiards with positive entropy*, Comm. Math. Phys. **141** (1991), 225–257.
- [FKCD] N. Friedman, A. Kaplan, D. Carasso, and N. Davidson, *Observation of Chaotic and Regular Dynamics in Atom-Optics Billiards*, Phys. Rev. Lett. **86** (2001), 1518–1521.
- [KS] A. Katok and J.-M. Strelcyn, *Invariant manifolds, entropy and billiards; smooth maps with singularities*, Lect. Notes Math., **1222**, Springer, New York (1986).
- [KMS] S. Kerckhoff, H. Masur, and J. Smillie, *Ergodicity of billiard flows and quadratic differentials*, Ann. Math. **124** (1986), 293–311.
- [L] V. F. Lazutkin, *On the existence of caustics for the billiard ball problem in a convex domain*, Math. USSR Izv. **7** (1973), 185–215.
- [M] R. Markarian, *Billiards with Pesin region of measure one*, Comm. Math. Phys. **118** (1988), 87–97.

- [S] Ya. G. Sinai, *Dynamical systems with elastic reflections. Ergodic properties of dispersing billiards*, Russ. Math. Surv. **25** (1970), 137–189.
- [Sz] D. Szász, *On the K-property of some planar hyperbolic billiards*, Comm. Math. Phys. **145** (1992), 595–604.
- [W] M. Wojtkowski, *Principles for the design of billiards with nonvanishing Lyapunov exponents*, Comm. Math. Phys. **105** (1986), 391–414.
- [Y] L.-S. Young, *Statistical properties of dynamical systems with some hyperbolicity*, Ann. Math. **147** (1998), 585–650.